

Impact of morphofunctional assessment with quantitative flow ratio and optical coherence tomography in patients with acute coronary syndromes

Yuto Osumi¹, MD; Hiroyuki Kawamori¹, MD, PhD; Takayoshi Toba¹, MD, PhD; Takashi Hiromasa¹, MD; Daichi Fujimoto¹, MD, PhD; Shunsuke Kakizaki¹, MD, PhD; Koichi Nakamura¹, MD, PhD; Tomoyo Hamana¹, MD, PhD; Hiroyuki Fujii¹, MD, PhD; Satoru Sasaki¹, MD, PhD; Seigo Iwane¹, MD; Tetsuya Yamamoto¹, MD; Shota Naniwa¹, MD; Yuki Sakamoto¹, MD; Koshi Matsuhama¹, MD; Yuta Fukuishi¹, MD; Amane Kozuki², MD, PhD; Junya Shite², MD, PhD; Tomofumi Takaya³, MD, PhD; Akihiko Ishida⁴, MD, PhD; Masamichi Iwasaki⁵, MD; Ken-ichi Hirata¹, MD, PhD; Hiromasa Otake^{1*}, MD, PhD

*Corresponding author: Department of Cardiology, Kobe University Graduate School of Medicine, 7-5-1 Kusunoki-cho, Chuo-ku, Kobe, Hyogo, 650-0017, Japan. E-mail: hotake@med.kobe-u.ac.jp

This paper also includes supplementary data published online at: <https://eurointervention.pcronline.com/doi/10.4244/EIJ-D-23-01043>

ABSTRACT

BACKGROUND: Combining morphological and physiological evaluations might improve the risk stratification of patients who undergo percutaneous coronary intervention (PCI) for acute coronary syndrome (ACS) culprit lesions.

AIMS: We aimed to investigate the clinical utility of morphofunctional evaluation after PCI for identifying ACS patients with increased risk of subsequent clinical events.

METHODS: We retrospectively studied 298 consecutive ACS patients who had undergone optical coherence tomography (OCT)-guided PCI. We performed OCT-based morphological analysis and quantitative flow ratio (QFR)-based physiological assessment immediately after PCI. The non-culprit segment (NCS) was defined as the most stenotic untreated segment in the culprit vessel. The primary outcome was target vessel failure (TVF), a composite of cardiac death, target vessel-related myocardial infarction, and ischaemia-driven target vessel revascularisation.

RESULTS: During a median follow-up period of 990 days, 42 patients experienced TVF. Cox regression analysis revealed that the presence of thin-cap fibroatheroma (TCFA) in the NCS and a low post-PCI QFR, or the presence of TCFA in the NCS and a high Δ QFR in the NCS (QFR_{NCS}), were independently associated with TVF. The subgroup with TCFA in the NCS and a low post-PCI QFR had a significantly higher incidence of TVF (75%) than the other subgroups, and those with TCFA in the NCS and a high Δ QFR_{NCS} had a significantly higher incidence of TVF (86%) than the other subgroups. The integration of TCFA in NCS, post-PCI QFR, and Δ QFR_{NCS} with traditional risk factors significantly enhanced the identification of subsequent TVF cases.

CONCLUSIONS: Combining post-PCI OCT and QFR evaluation may enhance risk stratification for ACS patients after successful PCI, particularly in predicting subsequent TVF.

KEYWORDS: ACS/NSTE-ACS; clinical research; fractional flow reserve; optical coherence tomography

Optical coherence tomography (OCT) provides high-resolution imaging for stent optimisation during percutaneous coronary intervention (PCI)¹. Residual ischaemia correlates with poorer clinical outcomes². However, PCI adequacy is predominantly evaluated through OCT-based morphology, often without physiological assessment, especially in patients with acute coronary syndrome (ACS). OCT detects vulnerable plaques like thin-cap fibroatheroma (TCFA), which predict future cardiovascular events. Yet, relying solely on OCT morphology lacks sufficient positive predictive value, necessitating further refinement.

Fractional flow reserve (FFR) is a common method for evaluating myocardial ischaemia. Previous studies consistently demonstrated that post-PCI FFR can predict long-term cardiovascular events in chronic coronary syndrome (CCS) patients². Quantitative flow ratio (QFR), an angiographically derived alternative to wire-based FFR, has emerged recently. Previous trials have demonstrated that QFR agrees with FFR measurements³. Based on these findings, we hypothesised that combining morphological plaque assessment using OCT and physiological assessment using QFR might improve the risk stratification of patients who undergo PCI for ACS culprit lesions. Thus, we conducted this study to investigate the clinical utility of morphofunctional evaluation after PCI for identifying ACS patients with an increased risk of subsequent clinical events.

Editorial, see page e908

Methods

STUDY POPULATION

This study included patients with ACS who had undergone OCT-guided PCI for *de novo* native lesions with drug-eluting stents between January 2010 and October 2020 at 5 institutions. The exclusion criteria were (1) left main trunk artery lesion, (2) cases without analysable OCT imaging, (3) cases with a final Thrombolysis in Myocardial Infarction grade <3, (4) lesions involving the right coronary artery ostium, (5) patients with atrial fibrillation, (6) patients with cardiac shock, (7) cases with poor angiogram quality for QFR, and (8) patients without at least 6 months of follow-up. Participating institutions and detailed definitions of ACS are provided in **Supplementary Appendix 1** and **Supplementary Appendix 2**.

The study protocol complied with the Declaration of Helsinki and was approved by the Ethics Committee of Kobe University Hospital. Informed consent was obtained as an opt-out on the Division of Cardiovascular Medicine website at Kobe University Graduate School of Medicine. The study was registered in the University Hospital

Impact on daily practice

The present study demonstrated that adding the presence of thin-cap fibroatheroma in the non-culprit segment (NCS), post-percutaneous coronary intervention quantitative flow ratio (QFR), and Δ QFR in the NCS to traditional risk factors significantly improved the discriminatory and reclassification abilities for identifying patients with subsequent target vessel failure (TVF). Our results suggested that morphofunctional assessments using optical coherence tomography and QFR allow the identification of patients with acute coronary syndrome at an increased risk of subsequent TVF after PCI.

Medical Information Network Clinical Trials Registry (UMIN000047675).

OPTICAL COHERENCE TOMOGRAPHY IMAGING ANALYSIS AND DEFINITIONS

We retrospectively collected the OCT images from a frequency-domain OCT system (ILUMIEN [Abbott]) at the end of the procedure. Details of the OCT image acquisition technique are described in **Supplementary Appendix 3**.

The OCT images were analysed for every cross-section over the entire length of the target segment. The target vessel segment was divided into the following longitudinal subsegments: (1) stented segment, (2) adjacent reference segment (≤ 5 mm in length), and (3) non-culprit segment (NCS) (**Figure 1**). The NCS was defined as the most stenotic untreated segment, with 30-70% area stenosis outside the stented segment in the entire OCT pullback analysis. The lumen area measurements were obtained in every frame at 0.1 mm or 0.2 mm intervals.

A qualitative assessment was performed to evaluate the presence of irregular in-stent protrusion, thrombus, malapposition, stent edge dissection, lipid-rich plaque (LRP), and TCFA. The details of the OCT analysis are presented in **Supplementary Appendix 3**.

POST-PCI QUANTITATIVE FLOW RATIO COMPUTATIONAL ANALYSIS

QFR was computed offline using the three-dimensional (3D) software package QAngio XA 3D (Medis Medical Imaging). 3D quantitative coronary angiography (3D-QCA) data were readily available.

Post-PCI QFR was calculated for the target vessel, and Δ QFR in the NCS (QFR_{NCS}) was calculated in the same vessel. ΔQFR_{NCS} represents the pressure gradients at the

Abbreviations

ACS acute coronary syndrome
FFR fractional flow reserve
LRP lipid-rich plaque
MLA minimum lumen area
NCS non-culprit segment
OCT optical coherence tomography

PCI percutaneous coronary intervention
QFR quantitative flow ratio
TCFA thin-cap fibroatheroma
TVF target vessel failure
TVR target vessel revascularisation

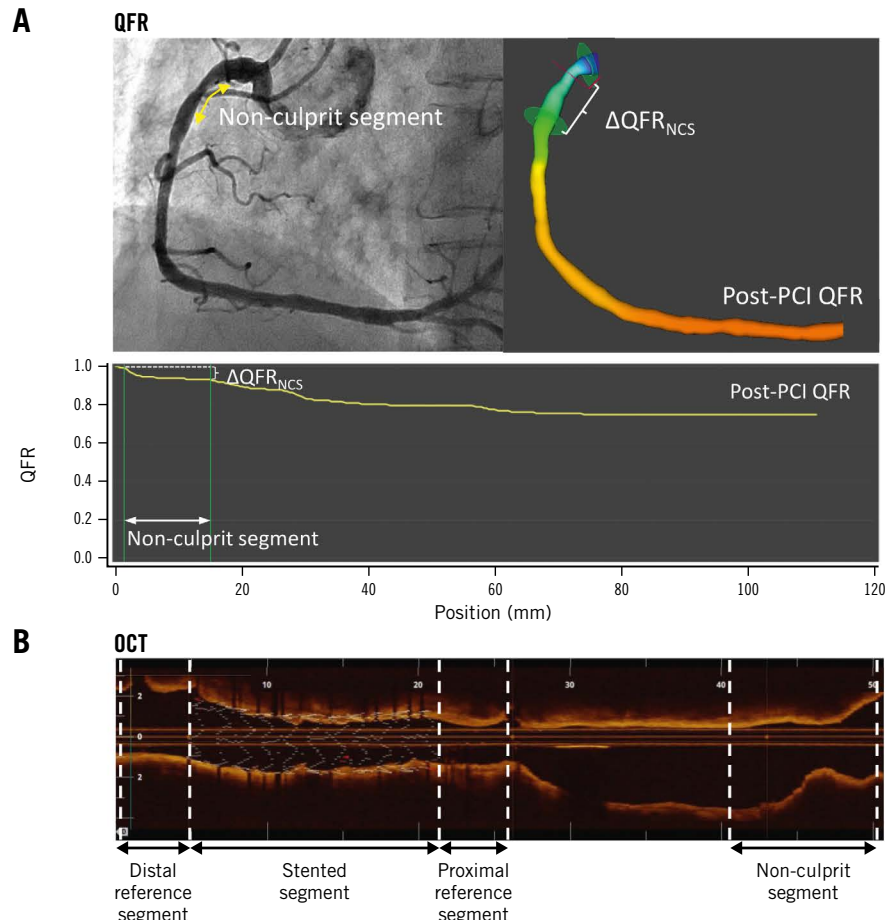


Figure 1. Subsegments analysed by QFR and OCT. A) QFR (the NCS is indicated with a yellow arrow; the white bracket indicates ΔQFR_{NCS}) and B) OCT showing (1) stented segment; (2) adjacent reference segment (≤ 5 mm); (3) non-culprit segment. NCS: non-culprit lesion; OCT: optical coherence tomography; PCI: percutaneous coronary intervention; QFR: quantitative flow ratio; QFR_{NCS} : QFR in the NCS

NCS (Figure 1). Details of the QFR analysis are presented in **Supplementary Appendix 4**.

OUTCOMES AND STATISTICAL ANALYSIS

The primary outcome was target vessel failure (TVF), defined as a composite of cardiac death, target vessel-related myocardial infarction (MI), and ischaemia-driven target vessel revascularisation (TVR). We further assessed non-target lesion revascularisation (TLR) TVR to evaluate the relationship between NCS-related findings and non-TLR TVR separately. Further details of the outcomes and statistical analyses are described in **Supplementary Appendix 5** and **Supplementary Appendix 6**.

Results

STUDY POPULATION

In total, 456 consecutive patients underwent OCT-guided PCI for ACS during the study period. After excluding 158 patients, 298 patients with 298 vessels were enrolled in this study (**Supplementary Figure 1**). All vessels had the NCS outside the stent segments, with a median artery length of 26.7 (interquartile range [IQR] 18-36) mm, which was not

significantly different between the TVF and non-TVF groups. The mean % diameter stenosis (DS) by 3D-QCA of the NCS was $21.5 \pm 12.1\%$. Baseline patient, lesion, and procedural characteristics are shown in **Table 1**. Post-PCI 3D-QCA, QFR, and OCT findings are shown in **Table 2** and **Table 3**. The distribution of post-PCI QFR is shown in **Supplementary Figure 2**, with a median value of 0.96 (IQR 0.91-0.98).

CLINICAL OUTCOME

During the median follow-up period of 990 (IQR 700-1,350) days after PCI, 42 (14%) patients experienced TVF. This included 9 (3%) patients who had cardiac death, 3 (1%) patients who experienced target vessel-related MI, and 34 (11%) patients who experienced TVR (**Supplementary Table 1**).

The median value of QFR at the time of the TVR event was significantly lower than that at the time of primary PCI (0.69 vs 0.85; $p < 0.001$), and the median value of lesion-level ΔQFR_{NCS} at the time of the TVR event was significantly higher than that at the time of primary PCI (0.18 vs 0.06; $p < 0.001$) (**Supplementary Figure 3**). Further details and a representative case of TVF are shown in **Supplementary Figure 4**.

Table 1. Baseline characteristics.

	Overall (n=298)	TVF (n=42)	Non-TVF (n=256)	p-value
Age, years	66±12	66±13	66±12	0.63
Male	227 (76)	30 (71)	197 (77)	0.44
Hypertension	194 (65)	26 (62)	168 (66)	0.64
Diabetes mellitus	112 (38)	16 (38)	96 (38)	0.94
Dyslipidaemia	197 (66)	24 (57)	173 (68)	0.19
Haemodialysis	4 (1)	2 (5)	2 (1)	0.04
Smoker	177 (59)	25 (60)	152 (59)	0.98
Family history	60 (20)	14 (33)	46 (18)	0.02
ACS				0.31
STEMI	194 (65)	28 (67)	166 (65)	
NSTEMI	62 (21)	11 (26)	51 (20)	
uAP	42 (14)	3 (7)	39 (15)	
Laboratory data				
eGFR, mL/min/1.73 m ²	72.0±18	70.9±23	71.7±17	0.78
Peak CK, IU/L	1,275 (347-2,579)	1,246 (399-2,863)	326 (1,275-2,513)	0.42
Peak CK-MB, IU/L	123 (26-270)	110 (30-260)	123 (24-271)	0.71
LVEF, %	54.3±10.4	50.3±11.5	55.0±10.1	0.007
Medication at discharge				
Statin	286 (96)	39 (93)	247 (96)	0.27
β-blocker	191 (64)	32 (76)	159 (62)	0.08
Lesion characteristics				
Vessel location				0.68
LAD	171 (57)	26 (62)	145 (57)	
LCx	32 (11)	3 (7)	29 (11)	
RCA	95 (32)	13 (31)	82 (32)	
Multivessel disease	107 (36)	23 (55)	84 (33)	0.006
Procedure				
Stent diameter, mm	3 (2.75-3.5)	3 (2.5-3)	3 (2.75-3.5)	0.33
Stent length, mm	24 (18-32)	28 (21-32)	24 (18-32)	0.41
Post-dilation	212 (71)	26 (62)	186 (73)	0.15

Values are expressed as mean±standard deviation, n (%) or median (25th-75th percentiles). ACS: acute coronary syndrome; CK: creatine kinase; CK-MB: creatine kinase-myocardial band; eGFR: estimated glomerular filtration rate; IU: international units; LAD: left anterior descending artery; LCx: left circumflex artery; LVEF: left ventricular ejection fraction; MI: myocardial infarction; NSTEMI: non-STEMI; PCI: percutaneous coronary intervention; RCA: right coronary artery; STEMI: ST-segment elevation myocardial infarction; TVF: target vessel failure; uAP: unstable angina pectoris

COMPARISONS BETWEEN THE TARGET VESSEL FAILURE AND NON-TARGET VESSEL FAILURE GROUPS

Patients in the TVF group had significantly higher frequencies of haemodialysis, family history of cardiovascular disease, and multivessel disease. They also had a significantly lower left ventricular ejection fraction (LVEF) than those in the non-TVF group (**Table 1**).

Regarding post-PCI 3D-QCA and QFR analysis, significantly higher %DS and lower post-PCI QFR in the entire vessel, as well as higher %DS and Δ QFR_{NCS} in the NCS, were observed in the TVF group than in the non-TVF group (**Table 2**).

Post-PCI OCT findings are shown in **Table 3**. The TVF group had a significantly smaller minimum lumen area (MLA) in the target vessel than the non-TVF group. The in-stent MLA was significantly smaller in the stented segment, and the prevalence of irregular protrusions and thrombus was

significantly higher in the TVF group than in the non-TVF group. The prevalence of suboptimal stent deployment was not significantly different between the 2 groups (p=0.49).

Regarding OCT findings of the reference segment, the TVF group had a significantly higher frequency of stent edge dissection, thrombus, LRP, and TCFA at the proximal reference than the non-TVF group.

Regarding the OCT findings of the NCS, the TVF group had significantly longer lesion lengths and smaller MLA than the non-TVF group. The frequencies of LRP and TCFA were significantly higher in the TVF group than in the non-TVF group.

FACTORS ASSOCIATED WITH TARGET VESSEL FAILURE

The results of univariate and multivariate Cox regression analyses for clinical factors, QFR, and OCT findings

Table 2. Post-PCI physiological indices.

	Overall (n=298)	TVF (n=42)	Non-TVF (n=256)	p-value
Entire target vessel				
MLD, mm	1.8±0.5	1.7±0.5	1.8±0.5	0.10
Diameter stenosis, %	34.2±9.8	41.1±12.4	33.1±8.8	<0.001
Post-PCI QFR	0.96 (0.91-0.98)	0.86 (0.73-0.94)	0.96 (0.91-0.98)	<0.001
Non-culprit lesion				
MLD, mm	2.4±0.6	2.0±0.6	2.4±0.5	<0.001
Diameter stenosis, %	21.5±12.1	32.0±13.6	19.7±11.1	<0.001
ΔQFR _{NCS}	0.006 (0-0.027)	0.06 (0.020-0.080)	0.004 (0-0.018)	<0.001

Values are expressed as mean±standard deviation or median (25th-75th percentiles). MLD: minimum lumen diameter; NCS: non-culprit segment; PCI: percutaneous coronary intervention; QFR: quantitative flow ratio; QFR_{NCS}: QFR in the NCS; TVF: target vessel failure

Table 3. Post-PCI OCT findings.

	Overall (n=298)	TVF (n=42)	Non-TVF (n=256)	p-value
Target vessel				
Length, mm	51.9±12.8	53.3±11.5	50.5±15.0	0.47
MLA, mm ²	3.9±2.3	2.8±1.8	4.0±2.4	<0.001
Stented segment				
Average lumen area, mm ²	6.8±2.1	6.3±2.5	6.8±2.1	0.18
MLA, mm ²	5.2±1.7	4.7±1.8	5.2±1.7	0.049
Lumen expansion, %	80.5±17.4	79.0±17.7	77.7±16.7	0.65
Irregular protrusion	143 (48)	29 (69)	114 (44)	0.003
Thrombus	84 (34)	21 (50)	63 (25)	<0.001
Malapposition	56 (23)	10 (24)	46 (18)	0.37
Suboptimal stent deployment	177 (59)	27 (64)	150 (59)	0.49
Reference segment				
Proximal reference				
Mean lumen area, mm ²	7.8±2.9	7.1±3.2	8.0±2.8	0.06
Stent edge dissection	15 (5)	5 (12)	10 (3)	0.028
Thrombus	32 (11)	10 (24)	22 (9)	0.003
LRP	65 (22)	16 (38)	49 (19)	0.006
TCFA	13 (4)	5 (12)	8(3)	0.01
Distal reference				
Mean lumen area, mm ²	5.7±2.5	5.3±3.1	5.7±2.3	0.22
Stent edge dissection	13 (4)	3 (7)	10 (3)	0.34
Thrombus	21 (7)	5 (12)	16 (6)	0.18
LRP	34 (11)	7 (17)	27 (11)	0.25
TCFA	10 (3)	3 (7)	7 (3)	0.14
Mean reference lumen area, mm ²	6.8±2.3	6.2±2.8	6.9±2.2	0.07
Non-culprit segment				
Artery length outside stent segment, mm	26.7 (18-36)	26.4 (19.2-33.9)	26.8 (17.9-36.8)	0.80
Distance from stent, mm	16 (13-21)	16 (13-20)	18 (14-23.3)	0.10
Length, mm	9.5 (5.6-13.6)	14.2 (10.3-16.9)	8.4 (5.2-12.4)	<0.001
MLA, mm ²	5.0±2.6	3.9±2.6	5.2±2.5	0.004
Thrombus	14 (5)	3 (7)	11 (4)	0.42
LRP	100 (34)	23 (55)	77 (30)	<0.001
TCFA	27 (9)	11 (26)	16 (6)	<0.001

Values are expressed as mean±standard deviation, n (%) or median (25th-75th percentiles). LRP: lipid-rich plaque; MLA: minimum lumen area; OCT: optical coherence tomography; PCI: percutaneous coronary intervention; TCFA: thin-cap fibroatheroma; TVF: target vessel failure

associated with TVF are summarised in **Table 4** and **Supplementary Table 2**. Multivariate model 1 showed that LVEF, post-PCI QFR, MLA in the NCS, and TCFA levels in the NCS were independently associated with TVF. Multivariate model 2 also showed that $\Delta\text{QFR}_{\text{NCS}}$, thrombus levels in the stented segment, and TCFA levels in the NCS were independently associated with TVF. The MLA in the NCS was not associated with TVF.

Receiver operating characteristic analysis showed that the cutoff value of post-PCI QFR and $\Delta\text{QFR}_{\text{NCS}}$ for identifying patients with subsequent TVF were 0.88 (sensitivity: 57.1, specificity: 88.3, the area under the curve [AUC]: 0.783, 95% confidence interval [CI]: 0.70-0.87) and 0.046 (sensitivity: 61.9, specificity: 92.6, AUC: 0.790, 95% CI: 0.70-0.88), respectively (**Supplementary Figure 5**). The incidence of TVF according to post-PCI QFR, $\Delta\text{QFR}_{\text{NCS}}$, and TCFA in the NCS is summarised in **Supplementary Figure 6**. Furthermore, the vessel subgroup with TCFA in the NCS and a low post-PCI QFR had a significantly higher incidence of TVF (75%) than the other subgroups, and patients with TCFA in the NCS and a high $\Delta\text{QFR}_{\text{NCS}}$ had a significantly higher incidence of TVF (86%) than the other patients (**Central illustration**). Furthermore, those with TCFA in the NCS and a high $\Delta\text{QFR}_{\text{NCS}}$ had a significantly higher incidence of non-TLR TVR (43%). A detailed relationship between TCFA in the NCS and a high $\Delta\text{QFR}_{\text{NCS}}$ and non-TLR TVR is shown in **Supplementary Figure 7**.

DISCRIMINATORY DIAGNOSTIC ABILITY OF POST-PCI QFR AND $\Delta\text{QFR}_{\text{NCS}}$ TO IDENTIFY PATIENTS WITH SUBSEQUENT TARGET VESSEL FAILURE

The **Central illustration** shows Harrell's C-index, net reclassification index (NRI), and relative integrated discrimination index (IDI) values for the four models. Compared with model 1 (traditional risk factors: age, male sex, body mass index, comorbidities of hypertension, dyslipidaemia, diabetes mellitus, smoking, and chronic kidney disease), model 2 (model 1 plus presence of TCFA in the NCS) showed a higher discriminatory ability (C-index: 0.61 vs 0.67; $p=0.07$) and higher reclassification ability (NRI: 0.391; $p=0.005$; relative IDI: 0.059; $p=0.005$) in identifying patients with subsequent TVF. Compared with model 2, model 3 (model 2 plus post-PCI QFR) showed a significantly higher discriminatory ability (C-index: 0.67 vs 0.79; $p=0.002$) and higher reclassification ability (NRI: 0.98; $p=0.001$, relative IDI: 0.217; $p<0.001$). Compared with model 2, model 4 (model 2 plus $\Delta\text{QFR}_{\text{NCS}}$) showed a significantly higher discriminatory ability (C-index: 0.67 vs 0.82; $p<0.001$) and higher reclassification ability (NRI: 1.06; $p<0.001$, relative IDI: 0.262; $p<0.001$).

FACTORS ASSOCIATED WITH A LOW POST-PCI QFR (<0.88) AND A HIGH $\Delta\text{QFR}_{\text{NCS}}$ (>0.046)

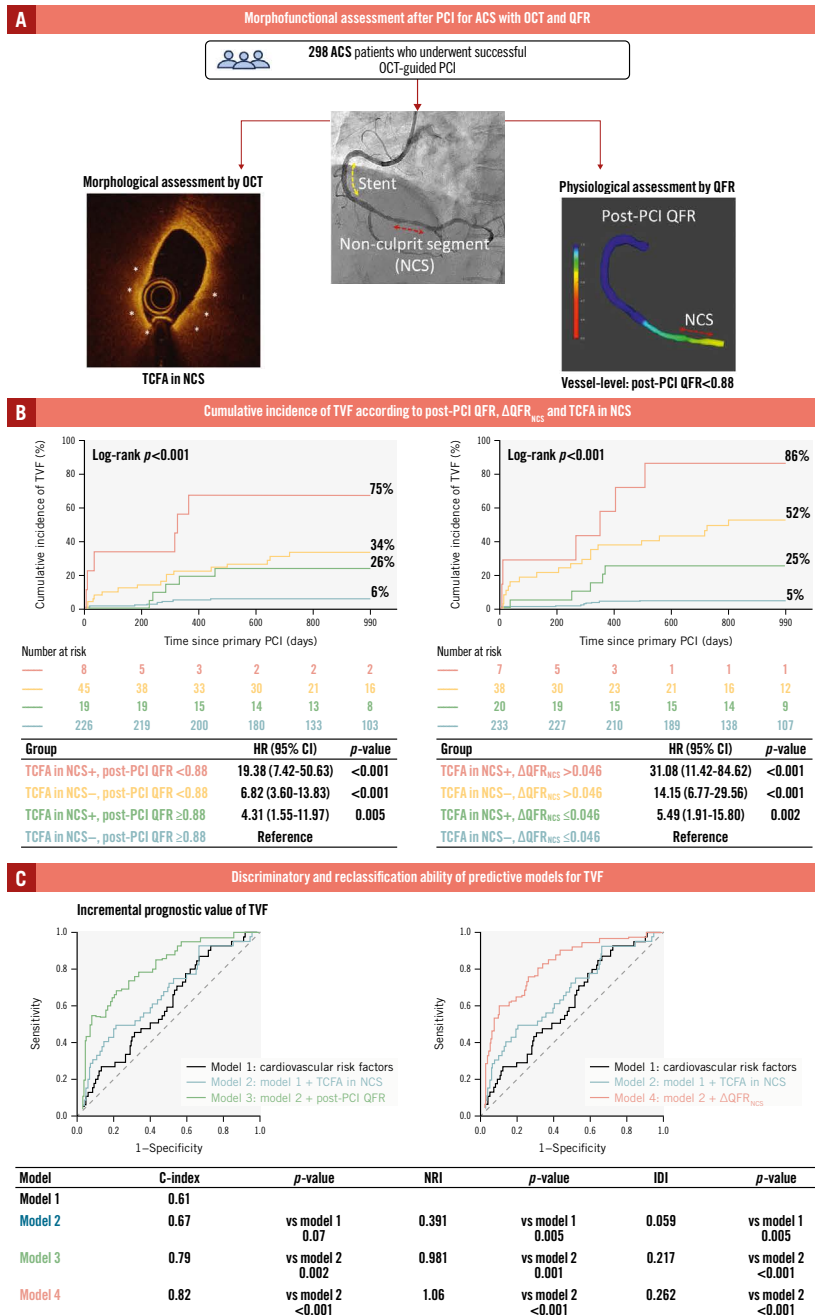
Multivariate logistic regression analysis showed that in-stent thrombus, stent edge dissection at the proximal reference,

Table 4. Multivariate Cox regression analyses of factors associated with TVF.

Variables	Multivariable			
	Model 1*		Model 2*	
	HR (95% CI)	p-value	HR (95% CI)	p-value
Baseline characteristics				
LVEF	0.97 (0.94-0.99)	0.01	0.99 (0.96-1.01)	0.31
Target vessel				
Post-PCI QFR (per 0.1 increase)	0.49 (0.39-0.62)	<0.001		
Stented segment				
Thrombus	1.42 (0.72-2.79)	0.32	1.85 (0.94-3.63)	0.07
Reference segment				
Stent edge dissection at proximal reference	0.94 (0.35-2.49)	0.91	1.85 (0.40-2.93)	0.87
Non-culprit lesion				
$\Delta\text{QFR}_{\text{NCS}}$ (per 0.01 increase)			1.15 (1.10-1.21)	<0.001
MLA	0.82 (0.71-0.96)	0.01	0.88 (0.75-1.03)	0.12
LRP	0.97 (0.44-2.15)	0.93	1.29 (0.60-2.76)	0.51
TCFA	4.15 (1.67-10.3)	0.002	3.47 (1.46-8.24)	0.005

HR corresponds to an increase of 0.1, 0.01 unit for each variable except for QFR, $\Delta\text{QFR}_{\text{NCS}}$. *We used 2 patterns of multivariable models based on the distinct qualities of post-PCI QFR and $\Delta\text{QFR}_{\text{NCS}}$. CI: confidence interval; HR: hazard ratio; LRP: lipid-rich plaque; LVEF: left ventricular ejection fraction; MLA: minimum lumen area; NCS: non-culprit segment; PCI: percutaneous coronary intervention; QFR: quantitative flow ratio; QFR_{NCS} : QFR in the NCS; TCFA: thin-cap fibroatheroma; TVF: target vessel failure

Risk stratification of ACS patients by morphofunctional assessment using OCT and QFR.



Yuto Osumi et al. • EuroIntervention 2024;20:e927-e936 • DOI: 10.4244/EIJ-D-23-01043

A) The NCS was an untreated, non-significantly stenotic segment outside the stented segment. * indicates presence of TCFA. The yellow dotted arrow indicates the stent location. The red dotted arrow indicates the location of the NCS. B) The vessel subgroup with TCFA in NCS and a low post-PCI QFR had a higher incidence of TVF (75%) than the other subgroups, and patients with TCFA in NCS and a high ΔQFR_{NCS} had a higher incidence of TVF (86%) than the other patients. C) Integration of TCFA in NCS, post-PCI QFR and ΔQFR_{NCS} with traditional risk factors improved discriminatory and reclassification ability in identifying patients with subsequent TVF. ACS: acute coronary syndrome; CI: confidence interval; HR: hazard ratio; IDI: integrated discrimination index; NCS: non-culprit segment; NRI: net reclassification index; OCT: optical coherence tomography; PCI: percutaneous coronary intervention; QFR: quantitative flow ratio; QFR_{NCS} : QFR in the NCS; TCFA: thin-cap fibroatheroma; TVF: target vessel failure

and lesion length of the NCS were independently associated with a low post-PCI QFR (<0.88). Moreover, lesion length and minimal lumen area at the NCS were independently associated with a high $\Delta\text{QFR}_{\text{NCS}}$ (>0.046) (**Supplementary Table 3**).

RELATIONSHIP BETWEEN NCS-RELATED FINDINGS AND NON-TLR TARGET VESSEL REVASCULARISATION

Among TVR cases, 19 patients experienced non-TLR TVR due to the development of a new lesion in the culprit vessel, as detailed in **Supplementary Table 1**. Regarding the relation between NCS findings and the location of non-TLR TVR, within the 19 non-TLR TVR cases, 15 occurrences (79%) were identified at the NCS site. Overall, there were 27 patients with TCFA in the NCS. Among them, 5 patients (19%) experienced non-TLR TVR, all of which occurred at the NCS site. Among 45 patients with a high $\Delta\text{QFR}_{\text{NCS}}$, 13 patients experienced non-TLR TVR, with 92% of these cases occurring at the NCS site. Furthermore, in the subset of patients presenting both TCFA in the NCS and a high $\Delta\text{QFR}_{\text{NCS}}$ (7 patients), 3 patients (43%) underwent non-TLR TVR, all of which were observed at the NCS site.

Comparisons between the non-TLR TVR group and other groups are presented in **Supplementary Table 4** and **Supplementary Table 5**. Multivariate Cox regression analyses showed that $\Delta\text{QFR}_{\text{NCS}}$, lesion length at the NCS, and TCFA in the NCS were independently associated with non-TLR TVR (**Supplementary Table 6**).

Discussion

The main findings of this study are as follows: (1) The TVF group had significantly worse physiological indices, including lower post-PCI QFR and higher $\Delta\text{QFR}_{\text{NCS}}$. (2) In addition to patient characteristics such as LVEF, the presence of TCFA in the NCS, a low post-PCI QFR, and a high $\Delta\text{QFR}_{\text{NCS}}$ were independently associated with TVF after PCI in patients with ACS. (3) Patients with a high $\Delta\text{QFR}_{\text{NCS}}$ and TCFA in the NCS had the highest TVF rate during a median follow-up of 990 days (86%) after PCI. (4) The addition of morphological OCT findings to cardiovascular risk factors increased the discriminant and reclassification abilities in the identification of subsequent TVF, which were further increased by adding post-PCI QFR or $\Delta\text{QFR}_{\text{NCS}}$. This real-world cohort study with long-term follow-up clarified the clinical utility of morphofunctional evaluation using QFR and OCT in identifying patients with subsequent TVF in patients with ACS after PCI.

IMPACT OF POST-PCI QFR MEASUREMENT IN PATIENTS WITH ACUTE CORONARY SYNDROME

Previous studies have consistently demonstrated that post-PCI FFR is a predictive marker for long-term cardiovascular events in patients with CCS². However, reliable physiological assessment during PCI can be challenging in patients with ACS because of microvascular dysfunction caused by capillary swelling and obstruction, distal embolisation, and vasoconstriction. Previous studies have shown elevated FFR values in both the culprit and non-culprit vessels in patients with ACS⁴, suggesting a potential underestimation of physiological lesion severity when measured during index PCI.

The QFR is a physiological index that can be calculated using angiographic data alone. Tang et al assessed the change in the QFR values of the culprit vessel from the index to the staged procedure in patients with ACS. They demonstrated that it is feasible to assess the QFR of culprit vessels immediately after the index PCI⁵.

Our study identified post-PCI QFR and $\Delta\text{QFR}_{\text{NCS}}$ as powerful independent risk factors for TVF. The Angio-Based Fractional Flow Reserve to Predict Adverse Events After Stent Implantation (HAWKEYE) trial demonstrated that post-PCI QFR was useful in predicting vessel-related cardiovascular events in patients with CCS and non-ST-elevation ACS. They also identified an optimal cutoff value of 0.89 for the post-PCI QFR⁶. Our study found that the optimal cutoff value for post-PCI QFR was 0.88, consistent with a previous report. These results highlight the significance of post-PCI QFR measurements in patients with ACS, providing a precise method for assessing the severity of residual physiological lesions and predicting clinical outcomes after PCI.

In addition to FFR, prior studies have already demonstrated an association between morphological evaluation of non-culprit lesions and subsequent adverse events. In the PROSPECT study, Stone et al demonstrated that MLA ($\leq 4 \text{ mm}^2$) in non-culprit lesions was an independent predictor of major adverse cardiovascular events (MACE) associated with non-culprit lesions in ACS patients⁷. However, in our study, MLA in the NCS was not associated with TVF when adjusted by $\Delta\text{QFR}_{\text{NCS}}$. Similarly, in the EMERALD study, Lee et al also demonstrated that the local pressure gradient (Δ computed tomography-derived FFR [FFR_{CT}]) had the highest discriminatory ability for subsequent coronary events compared to other indices, including %DS⁸, which is consistent with the results of our study. We currently speculate that the local physiological pressure gradient is a more important factor in plaque progression compared with single cross-sectional quantitative measurements such as MLA.

Furthermore, Takagi et al demonstrated an improved discrimination ability of translesional FFR_{CT} gradient compared to a standard diagnostic strategy of coronary CT angiography in predicting future revascularisation in patients with CCS⁹. On the other hand, our study focused not only on the prognostic potential of a high QFR gradient but also on elucidating the prognostic implications of morphofunctional assessment using QFR and OCT. Our results revealed that the combination of the presence of TCFA and translesional QFR gradient (or vessel-level QFR) significantly enhanced the accuracy of predicting TVF after PCI in patients with ACS. Of note, the median ΔQFR value of lesions with subsequent TVF was 0.06, with a cutoff value of 0.046 – considerably lower than those reported by Takagi et al (average translesional FFR_{CT} gradient: 0.24, cutoff: 0.13). However, when combined with the presence of TCFA, our approach demonstrated an approximately 80% TVF rate during the median follow-up of 990 days after the initial PCI. Although we acknowledge the need for confirmation through a future, prospective, large-scale study, we firmly believe that our data demonstrated the potential benefit of angio-based physiological assessment in predicting future clinical outcomes, especially when combined with morphological evaluation by OCT.

RELATIONSHIP BETWEEN THE COMBINED APPROACH OF QFR AND OCT AND CLINICAL OUTCOMES

Several studies have highlighted that the presence of TCFA on OCT is related to subsequent cardiac events in patients with coronary artery disease. In the recent prospective COMBINE OCT-FFR study, Kedhi et al investigated the impact of OCT-detected TCFA on the clinical outcomes of medically treated, angiographically intermediate, but FFR-negative patients with diabetes¹⁰. They demonstrated that TCFA-positive patients had a 5-fold higher rate of MACE despite the absence of ischaemia. However, the cumulative MACE rate was only 13.3% during the 18-month follow-up. In a recent single-centre retrospective study that enrolled 1,378 patients, Kubo et al demonstrated that OCT-based plaque characterisation is useful for detecting vulnerable plaques leading to ACS¹¹. However, the positive predictive values of LRPs and TCFA were limited to 11% and 19%, respectively.

Recently, several investigators have demonstrated the potential utility of combining morphological and physiological assessments to predict subsequent cardiac events. Hong et al conducted a retrospective study enrolling 604 patients with ACS who underwent OCT imaging in ≥ 1 non-culprit vessel during index coronary angiography¹². They demonstrated that a comprehensive morphofunctional evaluation of non-culprit vessels was significantly associated with the risk of non-culprit vessel-related MACE, identifying a subgroup of patients with a 43-fold higher risk of recurrent events at the 2-year follow-up. We also reported that adding OCT-derived FFR measurements to post-PCI morphological OCT findings in ACS culprit vessels better discriminated patients with subsequent TVF after PCI for ACS¹³. Although these studies implied the potential utility of combining morphological and physiological assessments over morphological evaluation alone, they calculated physiological indices from OCT images, limited the evaluation range to scanned segments, and excluded segments outside the range. In contrast, QFR enables physiological assessment of the entire vessel without additional procedures or adverse haemodynamic effects due to hyperaemia induction, which is needed for invasive FFR measurement.

QFR offers the advantage of providing vessel-level FFR measurements and enabling segmental physiological evaluation. In our study, we found that patients with TCFA in the NCS and a low post-PCI QFR (<0.88 : vessel-level analysis) had a 19.4-times higher risk of subsequent TVF, while those with TCFA in the NCS and a high $\Delta\text{QFR}_{\text{NCS}}$ (>0.046 : lesion-level analysis) had a 31.1-times higher risk of subsequent TVF. These findings suggest that lesion-level physiological assessments may be more effective than vessel-level physiological assessments for predicting subsequent cardiac events after PCI. Therefore, we recommend evaluating post-PCI QFR and $\Delta\text{QFR}_{\text{NCS}}$ simultaneously and considering additional procedures in patients with a high $\Delta\text{QFR}_{\text{NCS}}$.

In our study, the median $\Delta\text{QFR}_{\text{NCS}}$ value of lesions with TVF was 0.06, and the cutoff value for predicting TVF was 0.046, indicating that most such lesions were functionally non-significant immediately after PCI. Additionally, the prevalence of a combined high-risk phenotype (TCFA+high $\Delta\text{QFR}_{\text{NCS}}$) is very low (2%), and the positive predictive value of this finding for non-TLR TVR is limited to 43%. In a retrospective study enrolling patients with ACS who underwent OCT imaging

in ≥ 1 non-culprit vessel¹², Hong et al demonstrated that the presence of TCFA was 11%, and the revascularisation or MI rate was 17.2% in patients with TCFA during 24 months of follow-up. Moreover, Kubo et al demonstrated that OCT-based plaque characterisation is useful for TCFA leading to ACS, but the predictive value of this finding was limited to 19%¹¹. In our study, the presence of TCFA alone was 9%, and the cumulative non-TLR TVR rate was 18.5%, consistent with the previous reports. These findings suggest that even in ACS patients, the presence of TCFA in the culprit vessel is not very high, and the presence of TCFA does not always predict future adverse events. On the other hand, our study uniquely demonstrated that the presence of TCFA with a high $\Delta\text{QFR}_{\text{NCS}}$ was only 2%, but this combined approach dramatically increased the positive predictive value of non-TLR TVR (43%) compared with previous studies^{11,12}. Although our study does not provide a direct answer to the critical question of whether identification of or preventive treatment for vulnerable, functionally non-significant lesions alters the prognosis of patients, we firmly believe that our data illuminate the potential utility of such preventive measures. The ongoing VULNERABLE study (ClinicalTrials.gov: NCT05599061), a randomised comparison between PCI plus optimal medical therapy (OMT) and OMT alone for the treatment of FFR-negative vulnerable plaques, holds the promise of directly addressing this pivotal question.

Limitations

First, the study was retrospective; therefore, our results were subject to a selection bias. Specifically, including target vessel revascularisation as an endpoint introduces bias, as treating physicians might have been aware of the remaining lesions. Additionally, our results are subject to bias, because this study evaluated only the culprit vessels and could not evaluate non-culprit vessels, which may be associated with clinical outcomes. Furthermore, a prospective study is warranted to determine whether combining OCT and QFR can improve clinical outcomes. Second, the QFR measurements relied on angiographic images and optimal projections. Third, in the acute phase of ACS, factors like myocardial oedema, necrosis, inflammation, vasoconstriction, thrombus formation, or microembolisation during PCI may transiently affect microcirculatory vasodilation, potentially leading to underestimation of the physiological impact of stenotic lesions. This limitation may theoretically apply to QFR measurement in patients with ACS, as QFR simulation relies on an automated frame count for coronary flow assessment. Fourth, the sample size was small, particularly for patients with TCFA in the NCS and a low post-PCI QFR or a high $\Delta\text{QFR}_{\text{NCS}}$. Further large-scale studies are required to validate these findings.

Conclusions

Post-PCI physiological indices evaluated using QFR provide valuable information for patients with ACS risk stratification. Combining morphological and functional assessments using OCT and QFR allows the identification of patients with ACS at an increased risk of subsequent TVF after PCI. Due to the retrospective nature of the current study, the results should be considered hypothesis-generating, and future prospective studies confirming these findings are needed.

Authors' affiliations

1. Division of Cardiovascular Medicine, Department of Internal Medicine, Kobe University Graduate School of Medicine, Kobe, Japan; 2. Division of Cardiovascular Medicine, Osaka Saiseikai Nakatsu Hospital, Osaka, Japan; 3. Division of Cardiovascular Medicine, Hyogo Prefectural Harima-Himeji General Medical Center, Himeji, Japan; 4. Department of Cardiology, Toyooka Public Hospital, Toyooka, Japan; 5. Department of Cardiology, Hyogo Prefectural Awaji Medical Center, Sumoto, Japan

Conflict of interest statement

The authors have no conflicts of interest to declare.

References

- Johnson NP, Tóth GG, Lai D, Zhu H, Açar G, Agostoni P, Appelman Y, Arslan F, Barbato E, Chen SL, Di Serafino L, Domínguez-Franco AJ, Dupouy P, Esen AM, Esen OB, Hamilos M, Iwasaki K, Jensen LO, Jiménez-Navarro MF, Katritsis DG, Kocaman SA, Koo BK, López-Palop R, Lorin JD, Miller LH, Muller O, Nam CW, Oud N, Puymirat E, Rieber J, Rioufol G, Rodés-Cabau J, Sedlis SP, Takeishi Y, Tonino PA, Van Belle E, Verna E, Werner GS, Fearon WF, Pijls NH, De Bruyne B, Gould KL. Prognostic value of fractional flow reserve: linking physiologic severity to clinical outcomes. *J Am Coll Cardiol*. 2014;64:1641-54.
- Agarwal SK, Kasula S, Hacıoğlu Y, Ahmed Z, Uretsky BF, Hakeem A. Utilizing Post-Intervention Fractional Flow Reserve to Optimize Acute Results and the Relationship to Long-Term Outcomes. *JACC Cardiovasc Interv*. 2016;9:1022-31.
- Tu S, Westra J, Yang J, von Birgelen C, Ferrara A, Pellicano M, Nef H, Tebaldi M, Murasato Y, Lansky A, Barbato E, van der Heijden LC, Reiber JHC, Holm NR, Wijns W; FAVOR Pilot Trial Study Group. Diagnostic Accuracy of Fast Computational Approaches to Derive Fractional Flow Reserve From Diagnostic Coronary Angiography: The International Multicenter FAVOR Pilot Study. *JACC Cardiovasc Interv*. 2016;9:2024-35.
- Cuculi F, De Maria GL, Meier P, Dall'Armellina E, de Caterina AR, Channon KM, Prendergast BD, Choudhury RP, Forfar JC, Kharbada RK, Banning AP. Impact of microvascular obstruction on the assessment of coronary flow reserve, index of microcirculatory resistance, and fractional flow reserve after ST-segment elevation myocardial infarction. *J Am Coll Cardiol*. 2014;64:1894-904.
- Tang J, Chu J, Hou H, Lai Y, Tu S, Chen F, Yao Y, Ye Z, Gao Y, Mao Y, Zhuang S, Liu X. Clinical implication of QFR in patients with ST-segment elevation myocardial infarction after drug-eluting stent implantation. *Int J Cardiovasc Imaging*. 2021;37:755-66.
- Biscaglia S, Tebaldi M, Brugaletta S, Cerrato E, Erriquez A, Passarini G, Ielasi A, Spitaleri G, Di Girolamo D, Mezzapelle G, Geraci S, Manfrini M, Pavasini R, Barbato E, Campo G. Prognostic Value of QFR Measured Immediately After Successful Stent Implantation: The International Multicenter Prospective HAWKEYE Study. *JACC Cardiovasc Interv*. 2019;12:2079-88.
- Stone GW, Maehara A, Lansky AJ, de Bruyne B, Cristea E, Mintz GS, Mehran R, McPherson J, Farhat N, Marso SP, Parise H, Templin B, White R, Zhang Z, Serruys PW; PROSPECT Investigators. A prospective natural-history study of coronary atherosclerosis. *N Engl J Med*. 2011;364:226-35.
- Lee JM, Choi G, Koo BK, Hwang D, Park J, Zhang J, Kim KJ, Tong Y, Kim HJ, Grady L, Doh JH, Nam CW, Shin ES, Cho YS, Choi SY, Chun EJ, Choi JH, Nørgaard BL, Christiansen EH, Niemen K, Otake H, Penicka M, de Bruyne B, Kubo T, Akasaka T, Narula J, Douglas PS, Taylor CA, Kim HS. Identification of High-Risk Plaques Destined to Cause Acute Coronary Syndrome Using Coronary Computed Tomographic Angiography and Computational Fluid Dynamics. *JACC Cardiovasc Imaging*. 2019;12:1032-43.
- Takagi H, Leipsic JA, McNamara N, Martin I, Fairbairn TA, Akasaka T, Nørgaard BL, Berman DS, Chinnaiyan K, Hurwitz-Koweek LM, Pontone G, Kawasaki T, Rønnow Sand NP, Jensen JM, Amano T, Poon M, Øvrehus KA, Sonck J, Rabbat MG, Mullen S, De Bruyne B, Rogers C, Matsuo H, Bax JJ, Douglas PS, Patel MR, Nieman K, Ihdahid AR. Translesional fractional flow reserve gradient as derived from coronary CT

improves patient management: ADVANCE registry. *J Cardiovasc Comput Tomogr*. 2022;16:19-26.

- Kedhi E, Berta B, Roleder T, Hermanides RS, Fabris E, IJsselmuiden AJJ, Kauer F, Alfonso F, von Birgelen C, Escaned J, Camaro C, Kennedy MW, Pereira B, Magro M, Nef H, Reith S, Al Nooryani A, Rivero F, Malinowski K, De Luca G, Garcia Garcia H, Granada JF, Wojakowski W. Thin-cap fibroatheroma predicts clinical events in diabetic patients with normal fractional flow reserve: the COMBINE OCT-FFR trial. *Eur Heart J*. 2021;42:4671-9.
- Kubo T, Ino Y, Mintz GS, Shiono Y, Shimamura K, Takahata M, Terada K, Higashioka D, Emori H, Wada T, Kashiwagi M, Tanimoto T, Tanaka A, Hozumi T, Akasaka T. Optical coherence tomography detection of vulnerable plaques at high risk of developing acute coronary syndrome. *Eur Heart J Cardiovasc Imaging*. 2021;22:1376-84.
- Hong H, Jia H, Zeng M, Gutiérrez-Chico JL, Wang Y, Zeng X, Qin Y, Zhao C, Chu M, Huang J, Liu L, Hu S, He L, Chen L, Wijns W, Yu B, Tu S. Risk Stratification in Acute Coronary Syndrome by Comprehensive Morphofunctional Assessment With Optical Coherence Tomography. *JACC Asia*. 2022;2:460-72.
- Kakizaki S, Otake H, Seike F, Kawamori H, Toba T, Nakano S, Tanimura K, Takahashi Y, Fukuyama Y, Fujimoto D, Nakamura K, Fujii H, Kozuki A, Shite J, Iwasaki M, Takaya T, Yamaguchi O, Hirata KI. Optical Coherence Tomography Fractional Flow Reserve and Cardiovascular Outcomes in Patients With Acute Coronary Syndrome. *JACC Cardiovasc Interv*. 2022;15:2035-48.

Supplementary data

- Supplementary Appendix 1.** Participating institutions.
- Supplementary Appendix 2.** Definitions of ACS.
- Supplementary Appendix 3.** OCT image analysis and definitions.
- Supplementary Appendix 4.** QFR analysis.
- Supplementary Appendix 5.** Outcomes.
- Supplementary Appendix 6.** Statistical analysis.
- Supplementary Table 1.** Clinical events.
- Supplementary Table 2.** Univariate Cox regression analyses of factors associated with TVF.
- Supplementary Table 3.** Logistic regression analyses for factors associated with low post-PCI QFR and high $\Delta\text{QFR}_{\text{NCS}}$.
- Supplementary Table 4.** Baseline characteristics between patients with and without non-TLR TVR.
- Supplementary Table 5.** Post-PCI physiological indices and post-PCI OCT findings between patients with and without non-TLR TVR.
- Supplementary Table 6.** Uni- and multivariate Cox regression analyses of factors associated with non-TLR TVR.
- Supplementary Figure 1.** Patient flowchart.
- Supplementary Figure 2.** Distribution of post-PCI QFR.
- Supplementary Figure 3.** Comparison of post-PCI QFR and QFR at the event in patients with TVR.
- Supplementary Figure 4.** A representative case of a patient with TVR at 10 months after PCI.
- Supplementary Figure 5.** Receiver operating characteristic curve analysis for identifying patients with subsequent TVF from post-PCI QFR and $\Delta\text{QFR}_{\text{NCS}}$.
- Supplementary Figure 6.** Cumulative incidence of TVF according to post-PCI QFR, $\Delta\text{QFR}_{\text{NCS}}$, and TCFA in NCS.
- Supplementary Figure 7.** Proportions and incidence of non-TLR TVR according to $\Delta\text{QFR}_{\text{NCS}}$ and TCFA in NCS.

The supplementary data are published online at:
<https://eurointervention.pconline.com/doi/10.4244/EIJ-D-23-01043>



Supplementary data

Supplementary Appendix 1. Participating institutions.

- 1) Kobe University, Kobe, Japan; Osaka
- 2) Saiseikai Nakatsu Hospital, Osaka, Japan
- 3) Hyogo Prefectural Harima-Himeji General Medical Center, Himeji, Japan
- 4) Toyooka Public Hospital, Toyooka, Japan
- 5) Hyogo Prefectural Awaji Medical Center, Sumoto, Japan

Supplementary Appendix 2. Definitions of ACS.

Acute coronary syndrome (ACS) includes ST-elevation myocardial infarction, non-ST-elevation myocardial infarction, and unstable angina pectoris, as specified in the Fourth Universal Definition of Myocardial Infarction guidelines. ST-elevation myocardial infarction was defined as continuous chest pain lasting > 30 min, arrival at the hospital within 12 h from the onset of symptoms, ST-segment elevation > 0.1 mV in > 2 contiguous leads or new left bundle branch block on a 12-lead electrocardiogram, and elevated levels of cardiac markers (creatinine kinase-myocardial band or troponin T/I). Non-ST-segment elevation myocardial infarction was defined as ischaemic symptoms in the absence of ST-segment elevation on electrocardiogram, with elevated levels of cardiac markers. Unstable angina pectoris was defined as newly developed/accelerating chest symptoms upon exertion or resting angina within 2 weeks. The culprit

lesion was identified based on coronary angiography, electrocardiography, or echocardiography results.

Supplementary Appendix 3. OCT image analysis and definitions.

Optical coherence tomography (OCT) was performed on patients with ACS after percutaneous coronary intervention (PCI). OCT images were acquired using a frequency-domain OCT system (ILUMIEN; Abbott Vascular, Santa Clara, CA, USA) equipped with a Dragonfly Optis OCT imaging catheter (Abbott Vascular). A 0.014-inch conventional standard guide wire was positioned distally in the target vessel, and the OCT catheter (C7 and C8 Dragonfly™, Abbott Vascular) was advanced to the distal end of the target lesion. For image acquisition, blood in the lumen was replaced with contrast medium or low-molecular-weight dextran. OCT was performed at the end of the procedure from as far distal as possible to the ostium of the ACS culprit vessels using an integrated automated pullback device at 12 or 36 mm/s. The images were digitally stored offline. Two independent investigators blinded to the angiographic and physiological characteristics, including the quantitative flow ratio (QFR), analysed the acquired OCT images using dedicated software (Light Lab Imaging Inc., Westford, MA, USA). Discordance between the two investigators was resolved by consensus.

Stent under-expansion was defined as an in-stent minimum lumen area of < 70% of the average reference lumen area. The in-stent irregular protrusion was defined as the protrusion of a

material with an irregular surface into the lumen between the stent struts. A thrombus was defined as a mass protruding into the lumen with significant attenuation behind the mass. When a thrombus could not be completely differentiated from an irregular protrusion, particularly within the stented segment, it was categorised as an irregular protrusion. As struts are sometimes buried within the intima, we only included in-stent protrusions with a maximal height of $\geq 100 \mu\text{m}$ for analysis. Malapposition was defined as struts clearly separated from the vessel wall by $\geq 0.2 \text{ mm}$. Stent edge dissection was defined as disruption of the luminal surface with a visible flap at the stent edge or 5-mm proximal and distal reference segments. A lipid-rich plaque was defined as a plaque with a maximum lipid arc $> 180^\circ$. Thin-cap fibroatheroma was defined as a plaque with a fibrous-cap thickness of $< 65 \mu\text{m}$ and a lipid arc of $\geq 90^\circ$. Suboptimal OCT stent deployment was defined as the presence of at least one stent under expansion, in-stent plaque/thrombus protrusion $\geq 500 \mu\text{m}$, malapposition $> 200 \mu\text{m}$, and stent edge dissection $\geq 200 \mu\text{m}$.

Supplementary Appendix 4. QFR analysis.

QFR was computed offline using the three-dimensional software package QAngio XA 3 dimensional (Medis Medical Imaging System, Leiden, Netherlands) by two well-trained investigators. First, two diagnostic angiographic images with a separation of at least 25° were selected. A three-dimensional reconstruction of the interrogated vessel, excluding its side branches, was performed. The fixed-flow QFR was computed using a fixed hyperaemic flow velocity derived from a

previous study. The contrast-flow QFR was computed using a modelled hyperaemic flow velocity based on thrombolysis in myocardial infarction frame count analysis. In this study, we utilised the contrast-flow QFR, which demonstrated higher diagnostic accuracy than the fixed-flow QFR.

Supplementary Appendix 5. Outcomes.

The primary outcome was target vessel failure, defined as a composite of cardiac death, target vessel-related myocardial infarction (MI), and ischaemia-driven target vessel revascularisation (TVR). Cardiac death was defined according to the ARC definition, in which a cardiac cause could not be excluded. Target vessel-related MI was defined as MI in the vessel treated with index PCI. Ischaemia-driven TVR was defined as reintervention driven by any lesion in the same vessel treated with the index PCI.

Clinical follow-up assessments were performed at the primary care institution every 1–3 months after discharge. Clinical outcomes were ascertained by reviewing medical records and confirmed through direct contact with the patients, their families, or physicians.

Supplementary Appendix 6. Statistical analysis.

Continuous variables were tested for normal distribution using the Kolmogorov–Smirnov test. The mean±standard deviation is presented for normally distributed data, and the median (IQR) is reported for non-normally distributed data. Categorical variables are presented as numbers and

percentages. Continuous variables were compared using Student's t-test or the Mann–Whitney U test, as appropriate. Pearson's chi-squared or Fisher's exact test was used to compare categorical variables.

Receiver operating characteristic (ROC) curve analysis was conducted to evaluate the optimal cut-off values of QFR-related parameters for predicting TVF after PCI. Kaplan–Meier analysis was used to calculate the cumulative incidence of TVF, and the log-rank test was used to compare between-group differences. Cox regression analysis was performed to identify independent predictors associated with TVF. After selecting clinically meaningful variables, we further narrowed down the variables based on their significance in bivariate tests associated with TVF and univariable Cox regression analysis. Ultimately, we selected LVEF, post-PCI QFR, in-stent thrombus, stent edge dissection at the proximal reference, $\Delta\text{QFR}_{\text{NCS}}$, MLA levels in the NCS, LRP levels in the NCS, and TCFA levels in the NCS as explanatory variables in the multivariable Cox regression analysis. The discriminatory and reclassification abilities of patients with subsequent TVF, the additive values of post-PCI OCT findings, and the physiological indices of cardiovascular risk factors were evaluated by comparing Harrell's C index, category-free net reclassification index (NRI), and integrated discrimination index (IDI). Similar analyses were conducted on the NCS to identify patients who underwent subsequent non-TLR TVR. All statistical analyses were performed using SPSS (version 25; IBM Inc., Armonk, NY, USA) and R version 4.0.3 (The R Foundation for Statistical Computing, Vienna, Austria).

Supplementary Table 1. Clinical events.

	Overall	Low post-PCI QFR	High ΔQFR_{NCS}	TCFA in the NCS
	(n = 298)	(n = 53)	(n = 45)	(n = 27)
Cardiac death, n (%)	9 (3)	4 (7)	6 (13)	1 (4)
Target vessel-related MI, n (%)	3 (1)	1 (2)	1 (2)	1 (4)
TVR, n (%)	34 (11)	19 (36)	20 (44)	10 (37)
Non-TLR TVR, n (%)	19 (6)	13 (25)	13 (29)	5 (19)
TLR, n (%)	15 (5)	6 (11)	7 (15)	5 (19)

MI, myocardial infarction; NCS, non-culprit segment; PCI, percutaneous coronary intervention; QFR, quantitative flow ratio; TCFA, thin-cap fibroatheroma; TLR, target lesion revascularisation; TVR, target vessel revascularisation

Supplementary Table 2. Univariate Cox regression analyses of factors associated with TVF.

Variables	Univariable	
	HR (95% CI)	P-value
Baseline patient characteristics		
Age, years	1.01 (0.98–1.03)	0.51
Male	0.74 (0.38–1.45)	0.38
Hypertension	0.84 (0.45–1.56)	0.58
Diabetes mellitus	1.02 (0.55–1.90)	0.96
Dyslipidaemia	0.64 (0.35–1.18)	0.15
Haemodialysis	3.66 (0.89–15.15)	0.07
Smoking	0.91 (0.49–1.69)	0.76
LVEF	0.96 (0.94–0.99)	0.008
Target vessel		
Post-PCI QFR (per 0.1 increase)	0.48 (0.39–0.58)	< 0.001
MLA	0.60 (0.47–0.78)	< 0.001
Stented segment		
MLA	0.82 (0.67–0.99)	0.048
Irregular protrusion	2.56 (1.32–4.89)	0.005
Thrombus	2.76 (1.51–5.05)	0.001
Reference segment		
Stent edge dissection at proximal reference	7.73 (1.86–32.12)	0.005
Thrombus at proximal reference	2.77 (1.35–5.64)	0.005
LRP at proximal reference	2.38 (1.28–4.44)	0.006
TCFA at proximal reference	3.48 (1.37–8.86)	0.009
Average reference lumen area, mm ²	0.86 (0.74–1.00)	0.052

Non-culprit lesion

$\Delta\text{QFR}_{\text{NCS}}$ (per 0.01 increase)	1.16 (1.12–1.21)	< 0.001
Length	1.11 (1.07–1.15)	< 0.001
MLA	0.81 (0.69–0.94)	0.006
LRP	2.69 (1.46–4.96)	0.001
TCFA	3.99 (2.01–7.95)	< 0.001

HR corresponds to an increase of 0.1, 0.01 unit for each variable except for QFR, $\Delta\text{QFR}_{\text{NCS}}$.

CI, confidence interval; HR, hazard ratio; other abbreviations as in Table 1, Table 2, and Table 3.

Supplementary Table 3. Logistic regression analyses for factors associated with low post-PCI QFR and high Δ QFR_{NCS}.

Variables	Low post-PCI QFR				High Δ QFR _{NCS}			
	Univariable		Multivariable		Univariable		Multivariable	
	OR (95% CI)	P-value	OR (95% CI)	P-value	OR (95% CI)	P-value	OR (95% CI)	P-value
Target vessel								
Stent diameter	0.99 (0.94–1.05)	0.8						
Stent length	0.96 (0.93–1.0)	0.03						
Stented segment								
MLA	0.98 (0.82–1.17)	0.80						
Lumen expansion	1.35 (0.24–7.70)	0.73						

Irregular protrusion	1.91 (1.20–3.58)	0.04		
Thrombus	2.31 (1.25-4.28)	0.008	1.72 (0.75-3.96)	0.21
Malapposition	1.36 (0.73–2.57)	0.34		
Reference segment				
Stent edge dissection at PR	6.04 (2.09–17.5)	< 0.001	4.46 (1.17–17.00)	0.03
Stent edge dissection at DR	2.14 (0.63–7.32)	0.22		
Thrombus at PR	2.79 (1.25–6.22)	0.01		
Thrombus at DR	1.96 (0.72–5.31)	0.19		
Average reference lumen area	0.99 (0.87–1.13)	0.90		

Non-culprit lesion

Length	1.14 (1.08–1.20)	< 0.001	1.13 (1.07–1.20)	< 0.001	1.13 (1.08–1.20)	< 0.001	1.11 (1.05–1.18)	< 0.001
MLA	0.82 (0.71–0.95)	0.007	0.89 (0.76–1.03)	0.11	0.73 (0.61–0.87)	< 0.001	0.76 (0.64–0.92)	0.004
Thrombus	3.78 (1.25–11.4)	0.02			1.57 (0.42–5.87)	0.50	1.78 (0.17–18.20)	0.63
TCFA	2.11 (0.87–5.13)	0.09	1.24 (0.45–3.44)	0.67	2.15 (0.85–5.42)	0.11	1.68 (0.61–4.63)	0.31

CI, confidence interval; DR, distal reference; LRP, lipid-rich plaque; MLA, minimum lumen area; NCS, non-culprit segment; OR, odds ratio; PR, proximal reference; QFR, quantitative flow ratio; TCFA, thin-cap fibroatheroma

Supplementary Table 4. Baseline characteristics between patients with and without non-TLR

TVR.

	Overall	Non-TLR TVR	Others	P-value
	(n = 298)	(n = 19)	(n = 279)	
Age, years	66±12	65±12	66±12	0.63
Male, n (%)	227 (76)	12 (63)	215 (77)	0.17
Hypertension, n (%)	194 (65)	13 (68)	181 (65)	0.75
Diabetes mellitus, n (%)	112 (38)	8 (42)	104 (37)	0.67
Dyslipidaemia, n (%)	197 (66)	11 (58)	186 (67)	0.43
Haemodialysis, n (%)	4 (1)	0 (0)	4 (1)	0.60
Smoking, n (%)	177 (59)	11 (58)	166 (59)	0.89
Family history, n (%)	60 (20)	8 (42)	52 (19)	0.014
STEMI/ NSTEMI/ uAP, n (%)	194 (65)/ 62(21)/ 42(14)	15 (79)/4 (21)/ 0(0)	179 (64)/ 58(21)/ 42 (15)	0.18
Laboratory data				
estimated GFR, ml/min/1.73m ²	72±18	69±15	72±18	0.44
Peak CK, IU/L	1275 (347–2579)	1192 (456–3297)	1278 (325–2554)	0.94
Peak CK-MB, IU/L	123 (26–270)	100 (36–254)	123 (26–272)	0.42
LVEF, %	54.3±10.4	54.7±7.8	54.3±10.6	0.88
Lesion characteristics				
Vessel location	171 (57)/ 32 (11)/	13 (68)/ 0 (0)/ 6	158 (57)/ 32	0.27
LAD/ LCx/ RCA, n (%)	95 (32)	(32)	(12)/ 89 (32)	
Multivessel disease	107 (36)	9 (47)	98 (35)	0.28

Values are expressed as average \pm standard deviation, median (25th, 75th percentiles) or n (%)

CK, creatine kinase; CK-MB, creatine kinase-myocardial band; LAD, left anterior descending artery; LCx, left circumflex artery; LVEF, left ventricular ejection fraction; MI, myocardial infarction; PCI, percutaneous coronary intervention; RCA, right coronary artery; STEMI, ST-segment elevation myocardial infarction; TLR, target lesion revascularisation; TVR, target vessel revascularisation; uAP, unstable angina pectoris.

Supplementary Table 5. Post-PCI physiological indices and post-PCI OCT findings between patients with and without non-TLR TVR.

	Overall	Non-TLR TVR	Others	P-value
	(n = 298)	(n = 19)	(n = 279)	
3D-QCA and Physiological indices				
MLD, mm	2.4±0.6	2.1±0.4	2.4±0.6	0.02
Diameter stenosis, %	21.5±21.5	32.4±11.8	20.7±11.8	< 0.001
ΔQFR _{NCS}	0.006	0.06	0.005	< 0.001
	(0–0.03)	(0.03–0.08)	(0–0.02)	
Post-PCI OCT findings at NCS				
Length, mm	10.1±5.7	15.4±3.6	9.7±5.6	0.002
MLA, mm ²	5.0±2.6	3.8±2.7	5.1±2.6	0.04
Thrombus, n (%)	14 (5)	2 (11)	12 (4)	0.22
LRP, n (%)	101 (34)	11 (58)	90 (32)	0.02
TCFA, n (%)	27 (9)	5 (26)	22 (8)	0.007

Values are expressed as average ± standard deviation, median (25th, 75th percentiles) or n (%)

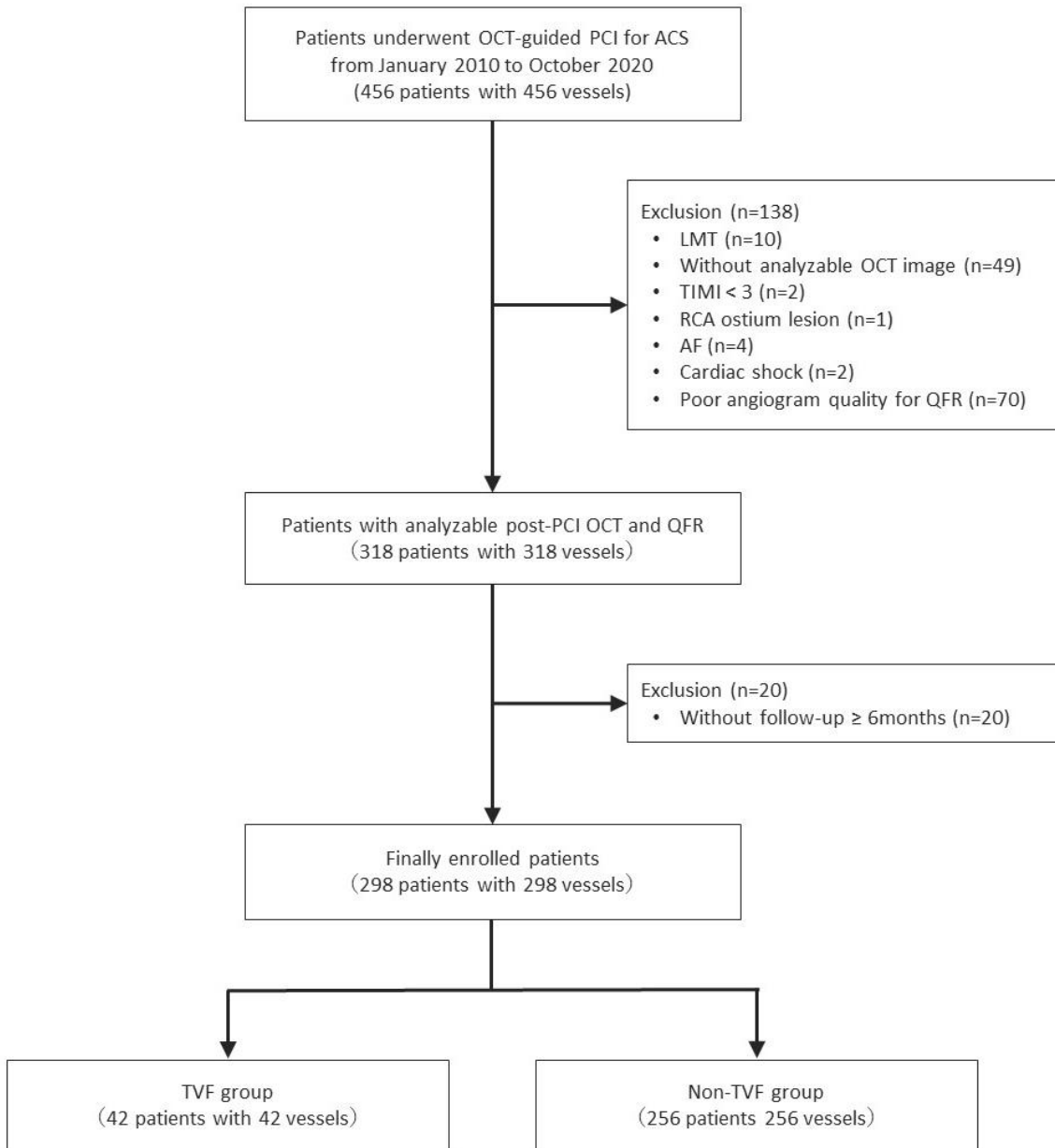
LRP, lipid-rich plaque; MLA, minimum lumen area; MLD, minimum lumen diameter; NCS, non-culprit segment; OCT, optical coherence tomography; PCI, percutaneous coronary intervention; 3D-QCA, three-dimensional quantitative coronary angiography; QFR, quantitative flow ratio; TCFA, thin-cap fibroatheroma; TLR, target lesion revascularisation; TVR, target vessel revascularisation.

Supplementary Table 6. Uni- and multivariate Cox regression analyses of factors associated with non-TLR TVR.

Variables	Univariable			Multivariable		
	HR	95% CI	P-value	HR	95% CI	P-value
Baseline patient characteristics						
Family history	0.99	0.96–1.03	0.76			
Non-culprit lesion						
Δ QFR _{NCS} (per 0.01 increase)	1.17	1.10–1.23	< 0.001	1.12	1.04–1.20	0.002
Length	1.12	1.07–1.19	< 0.001	1.07	1.00–1.15	0.036
MLA	0.76	0.60–0.97	0.02	0.87	0.69–1.11	0.27
LRP	2.70	1.09–6.71	0.033			
TCFA	3.66	1.32–10.16	0.013	3.83	1.30–11.27	0.015

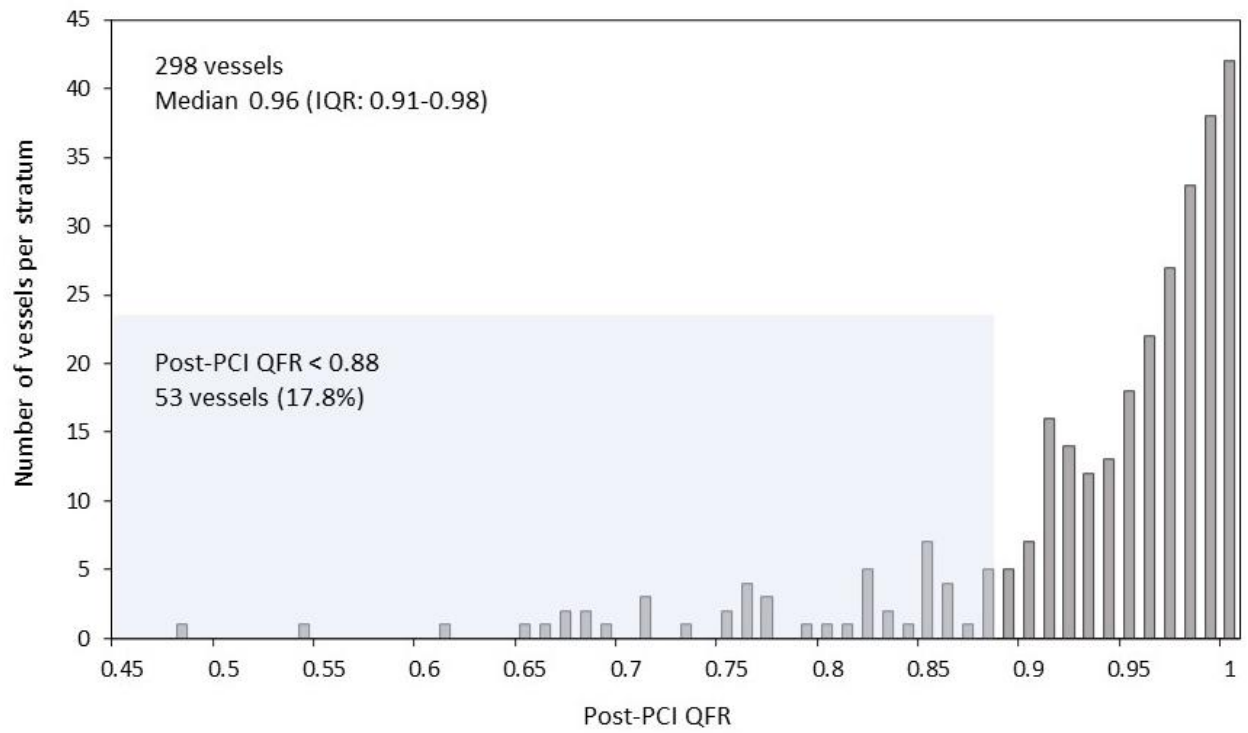
HR corresponds to an increase of 0.01 unit for each variable except for Δ QFR_{NCS}.

CI, confidence interval; HR, hazard ratio; LRP, lipid-rich plaque; MLA, minimum lumen area; NCS, non-culprit segment; QFR, quantitative flow ratio; TCFA, thin-cap fibroatheroma; TLR, target lesion revascularisation; TVR, target vessel revascularisation.



Supplementary Figure 1. Patient flowchart.

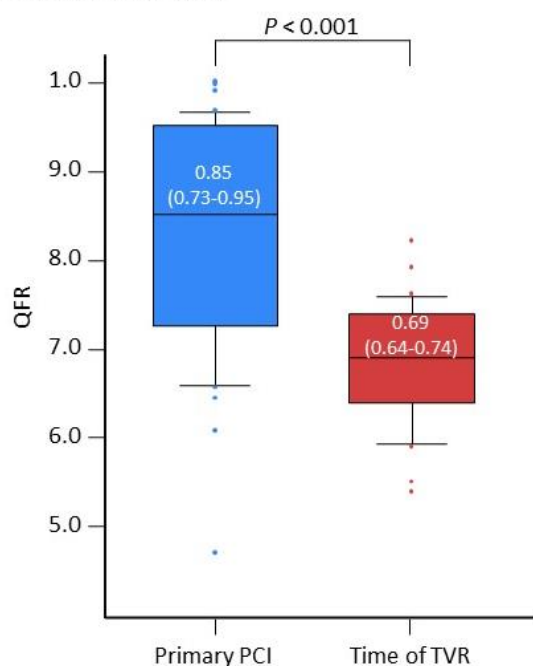
ACS, acute coronary syndrome; ISR, in-stent restenosis; LMT, left main trunk; OCT, optical coherence tomography; PCI, percutaneous coronary intervention; QFR, quantitative flow ratio; RCA, right coronary artery; TIMI, Thrombolysis in Myocardial Infarction; TVF, target vessel failure.



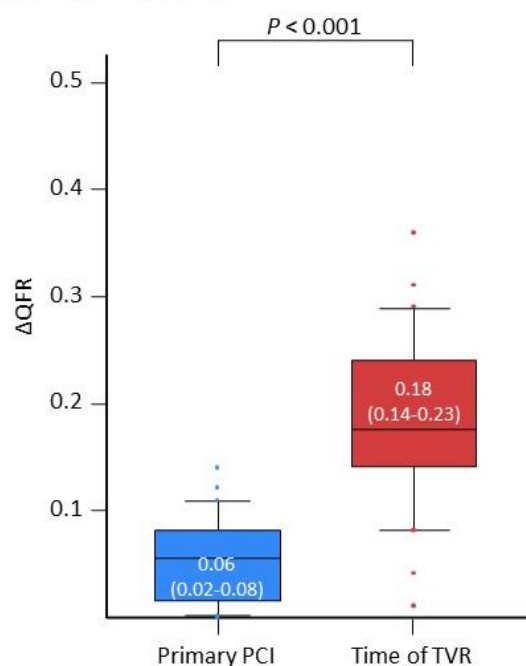
Supplementary Figure 2. Distribution of post-PCI QFR.

PCI, percutaneous coronary intervention; QFR, quantitative flow ratio

A. Vessel-level QFR



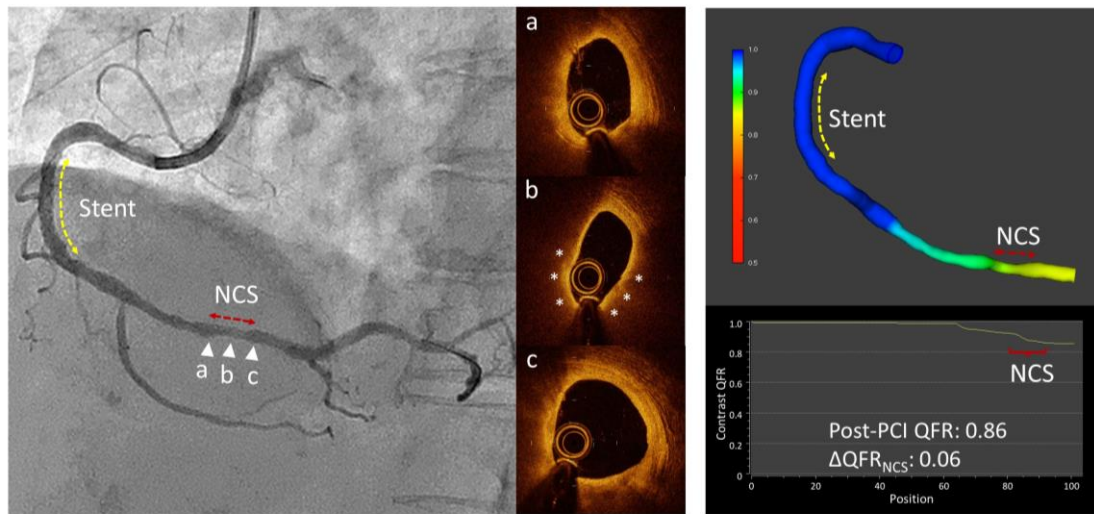
B. Lesion-level Δ QFR



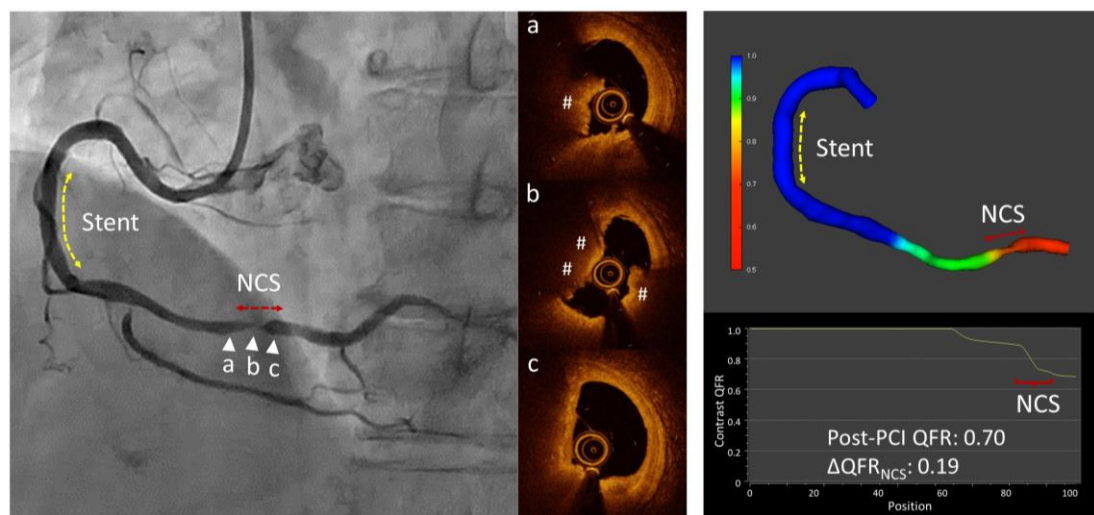
Supplementary Figure 3. Comparison of post-PCI QFR and QFR at the event in patients with TVR.

PCI, percutaneous coronary intervention; QFR, quantitative flow ratio; TVR, target vessel revascularisation.

A. CAG, OCT, and QFR immediately after PCI



B. CAG, OCT, and QFR at 10 months after PCI



Supplementary Figure 4. A representative case of a patient with TVR at 10 months after PCI.

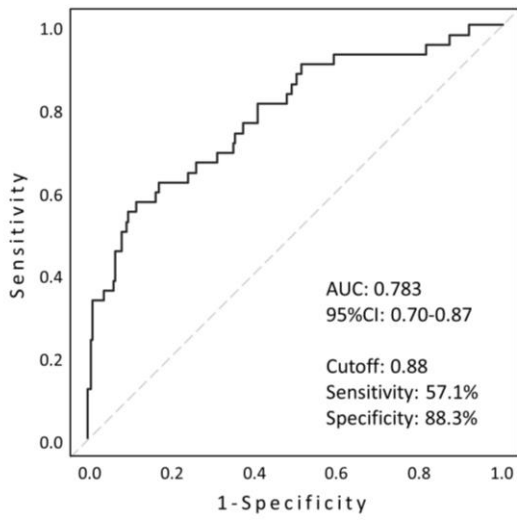
(A) An 85-year-old woman underwent percutaneous coronary intervention (PCI) with Xience Alpine 3.25*23 mm for a STEMI culprit lesion in the RCA. Post-PCI OCT image showing an in-stent MLA of 6.45 mm², irregular protrusion, and residual intermediate stenotic lesion with TCFA in the distal region of the stented segment (a-c). PCI was deferred during emergency PCI based on angiographic severity. The post-PCI QFR was 0.86, below the cut-off value of 0.88, and ΔQFR_{NCS} was 0.06,

higher than 0.046. * indicates TCFA.

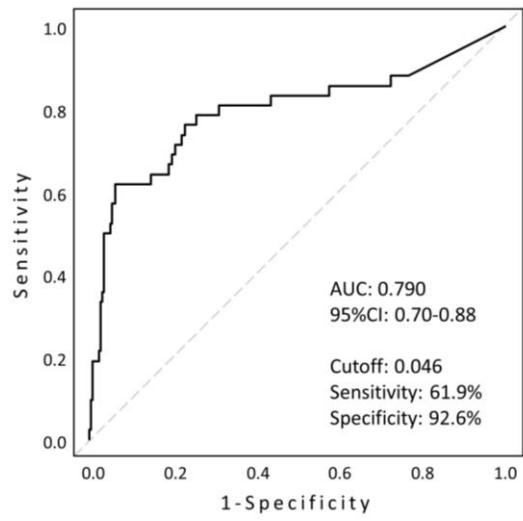
(B) Ten months later, the patient experienced chest pain during exertion. Urgent CAG revealed severe angiographic stenosis of the residual intermediate stenotic lesion with the TCFA. OCT images show the presence of a thrombus with significant narrowing. # indicates a thrombus.

CAG, coronary angiography; MLA, minimum lumen area; NCS, non-culprit segment; OCT, optical coherence tomography; PCI, percutaneous coronary intervention; QFR, quantitative flow ratio; RCA, right coronary artery; STEMI, ST-segment elevation myocardial infarction; TCFA, thin-cap fibroatheroma; TVF, target vessel revascularisation; TVR, target vessel revascularisation.

A. post-PCI QFR

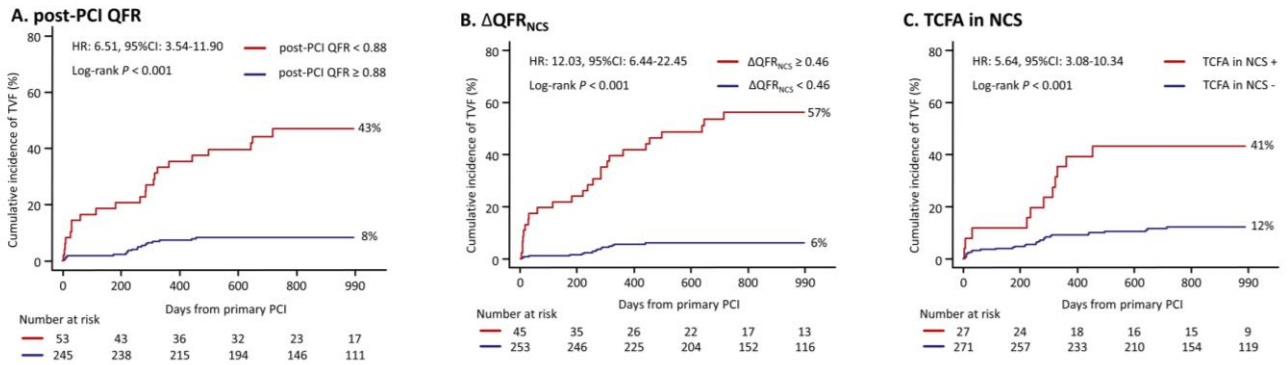


B. Δ QFR_{NCS}



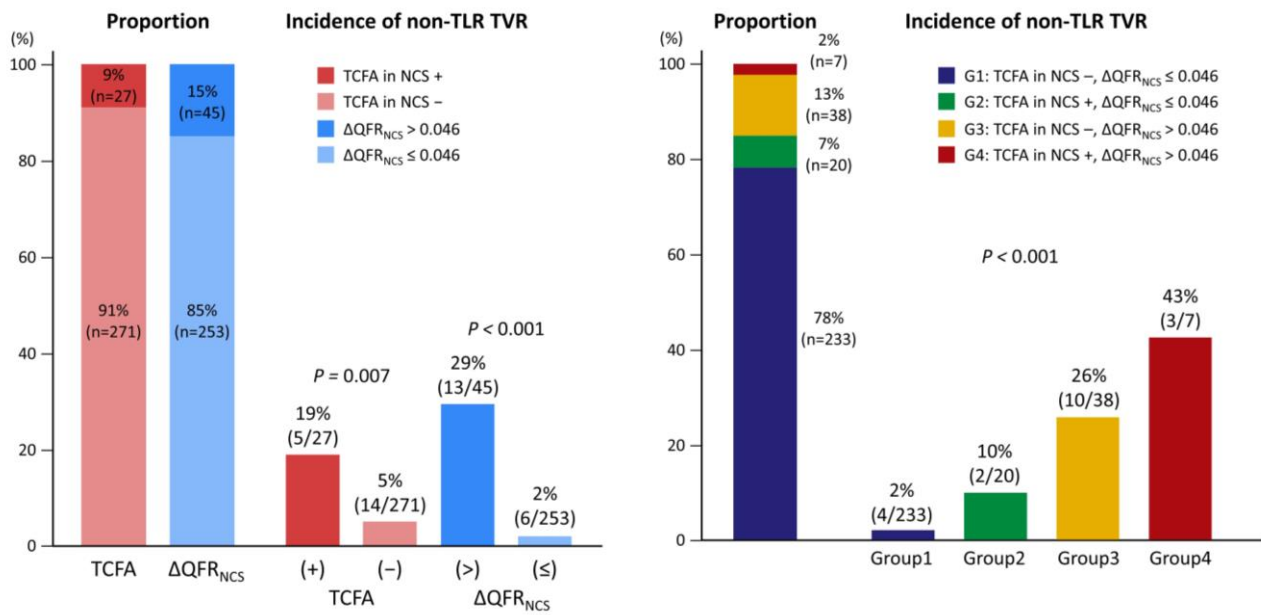
Supplementary Figure 5. Receiver operating characteristic curve analysis for identifying patients with subsequent TVF from post-PCI QFR and Δ QFR_{NCS}.

AUC, area under the curve; CI, confidence interval; NCS, non-culprit segment; PCI, percutaneous coronary intervention; QFR, quantitative flow ratio; TVF, target vessel failure.



Supplementary Figure 6. Cumulative incidence of TVF according to post-PCI QFR, ΔQFR_{NCS} , and TCFA in NCS.

(A) post-PCI QFR, (B) ΔQFR_{NCS} , and (C) TCFA in the NCS. HR, hazard ratio; NCS, non-culprit segment; PCI, percutaneous coronary intervention; QFR, quantitative flow ratio; TCFA, thin-cap fibroatheroma; TVF, target vessel failure.



Supplementary Figure 7. Proportions and incidence of non-TLR TVR according to ΔQFR_{NCS} and TCFA in NCS.

NCS, non-culprit segment; QFR, quantitative flow ratio; TCFA, thin-cap fibroatheroma; TLR, target lesion revascularisation; TVR, target vessel revascularisation.